AEDC-TDR-64-226

INVESTIGATION OF STING SUPPORT INTERFERENCE EFFECTS ON THE DYNAMIC AND STATIC STABILITY CHARACTERISTICS OF A 10-DEG CONE AT MACH NUMBERS 2.5, 3.0, AND 4.0

By

B. L. Uselton

von Kármán Gas Dynamics Facility

ARO, Inc.

TECHNICAL DOCUMENTARY REPORT NO. AEDC-TDR-64-226

November 1964

Program Element 62405634/8219, Task 821902

ARNOLD ENGINEERING DEVELOPMENT CENTER

AIR FORCE SYSTEMS COMMAND

UNITED STATES AIR FORCE

INVESTIGATION OF STING SUPPORT INTERFERENCE

EFFECTS ON THE DYNAMIC AND STATIC STABILITY

CHARACTERISTICS OF A 10-DEG CONE AT MACH

NUMBERS 2.5, 3.0, AND 4.0

By

B. L. Uselton

von Kármán Gas Dynamics Facility

ARO, Inc.

a subsidiary of Sverdrup and Parcel, Inc.
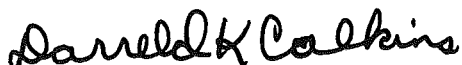
November 1964

ARO Project VT0357

ABSTRACT

Tests were conducted in Tunnel D of the von Kármán Gas Dynamics Facility to investigate sting support interference effects on the dynamic and static stability characteristics of a 10-deg half-angle cone. A free oscillation, cross-flexure pivot balance system was used.

Data were obtained at Mach numbers of 2.5, 3.0, and 4.0 at Reynolds numbers ranging from 0.45×10^6 to 10.2×10^6. Selected test results are presented, and comparisons are made with first- and second-order potential flow theory and conical flow theory.

PUBLICATION REVIEW

This report has been reviewed and publication is approved.

Darreld K. Calkins
Major, USAF
AF Representative, VKF
DCS/Test

Jean A. Jack
Colonel, USAF
DCS/Test

CONTENTS

TABLE

ILLUSTRATIONS

Figure   Page

NOMENCLATURE

A	Reference area (base area), in.^{2}
C_m	Pitching-moment coefficient, pitching moment/$q_\infty Ad$
C_{mq}	$\left[\partial C_m / \partial(qd/2V_\infty)\right]_{q \to 0}$
$C_{m\dot{\alpha}}$	$\left[\partial C_m / \partial(\dot{\alpha}d/2V_\infty)\right]_{\dot{\alpha} \to 0}$ } Damping-in-pitch derivatives, 1/rad
$C_{m\theta}$	Slope of the pitching-moment curve, 1/rad
C_{yR}	Cycles to damp to a given amplitude ratio, R, cycles
d	Reference length (model base diameter), in.
d_s	Diameter of sting, in.
f	Frequency of oscillation, cycles/sec
I	Model moment of inertia about the pivot axis, slug-ft^2
ℓ	Model length, in.
ℓn	Natural logarithm
ℓ_s	Distance from base of model to front edge of windshield, in.
M_θ	Angular restoring-moment parameter, ft-lb/rad
M'_θ	Aerodynamic angular restoring-moment parameter, ft-lb/rad
$M_{\dot{\theta}}$	Angular viscous-damping-moment parameter, ft-lb-sec/rad
$M'_{\dot{\theta}}$	Aerodynamic angular viscous-damping-moment parameter, ft-lb-sec/rad
M_∞	Nominal free-stream Mach number
p_b	Base pressure, psia
p_∞	Free-stream static pressure, psia
q	Pitching velocity, rad/sec
q_∞	Free-stream dynamic pressure, lb/ft^2
R	Ratio of amplitude of a damped oscillation after a given number of cycles to the initial amplitude
Re_ℓ	Reynolds number based on model length
r_b	Radius of model base, in.

r_n	Radius of model nose, in.
t	Time, sec
V_∞	Free-stream velocity, ft/sec
x_{cg}	Distance from model nose to pivot axis, in.
α	Angle of attack, rad or deg
$\dot{\alpha}$	Time rate of change of angle of attack, rad/sec
θ	Angular displacement, rad or deg
$\dot{\theta}$	Angular velocity, rad/sec
$\ddot{\theta}$	Angular acceleration, rad/sec^2
ω	Angular frequency, rad/sec
$\omega d/2V_\infty$	Reduced frequency parameter, rad

SUBSCRIPTS

o	Maximum conditions
v	Vacuum conditions
w	Wind-on conditions

1.0 INTRODUCTION

Tests were conducted during the period from June 29, 1964 to July 14, 1964 in the Gas Dynamic Wind Tunnel, Supersonic (D) of the von Kármán Gas Dynamics Facility (VKF), Arnold Engineering Development Center (AEDC), Air Force Systems Command (AFSC). These tests were in support of sting interference studies to be conducted in the VKF Mach 10 tunnel at the request of the Air Force Flight Dynamics Laboratory (AFFDL), AFSC, for the General Electric Missile and Space Division.

The Mach 10 interference studies will utilize a transverse-rod model support in conjunction with dummy stings to assess the interference effects of sting diameter and length. These data will be compared with data obtained with a sting support system (Ref. 1) in order to determine the relative interference effects of sting and transverse-rod supports. The objectives of the present tests were to supplement the tests in the Mach 10 tunnel by determining the effects of sting diameter and sting length on the damping-in-pitch derivatives ($C_{m_q} + C_{m_{\dot{\alpha}}}$) and on the slope of the pitching-moment curve (C_{m_θ}) at $M_\infty = 2.5$ through 4.0.

A low amplitude (±3 deg), free oscillation balance, incorporating a cross-flexure pivot, was used throughout the tests. Data were obtained on a 10-deg half-angle cone at Mach numbers 2.5, 3.0, and 4.0 at Reynolds numbers ranging from 0.45 x 10^6 to 10.2 x 10^6.

2.0 APPARATUS

2.1 WIND TUNNEL

Tunnel D (Fig. 1) is an intermittent, variable-density wind tunnel with a manually adjusted, flexible plate-type nozzle and a 12- by 12-in. test section. The tunnel operates at Mach numbers from 1.5 to 5 at stagnation pressures from about 5 to 60 psia and at stagnation temperatures up to about 80°F. A description of the tunnel and airflow calibration information may be found in Ref. 2.

2.2 MODEL

The model was a 10-deg half-angle cone constructed of aluminum, and provisions were made to add ballast to locate the model center of gravity exactly at the balance pivot axis. The model geometry is shown in Fig. 2.

Manuscript received October 1964.

2.3 STING-BALANCE SYSTEM

The dynamic stability balance (Fig. 3) is a one-degree-of-freedom, free oscillation, sting-supported system incorporating a cross-flexure as the pivot. The balance is designed for an initial displacement amplitude of about 3 deg. The model could be initially displaced, released, and locked from outside the tunnel by the manually operated cables shown in Fig. 3.

The basic sting diameter was 0.8 in. Three aluminum sleeves were used to provide the four sting diameter ratios (d_S/d = 0.2, 0.4, 0.6, and 0.8) to be used during the test. Windshields were also provided to slide along each sting to vary the sting length ratio from ℓ_s/d = 0.75 to 3.00. Figure 4 shows a typical model, sting, windshield arrangement installed in Tunnel D.

3.0 INSTRUMENTATION

The angular displacement of the model was monitored by a strain-gage bridge mounted on a side cross-flexure. A continuous time-resolved record of the outputs of the strain gage was obtained on a direct-writing oscillograph. The model base pressure was measured by means of an external pressure transducer. The tunnel D automatic data-handling system was used to tabulate tunnel parameters and the output of the pressure transducer.

4.0 PROCEDURE

The equations of motion for a free oscillation, one-degree-of-freedom system may be expressed as

$$I\ddot{\theta} - M_{\dot{\theta}}\dot{\theta} - M_{\theta}\theta = 0$$

The method for computing the dimensionless damping-in-pitch derivatives is indicated by the following expressions:

$$\theta = \theta_0 \, e^{(M_{\dot{\theta}}/2I)t} \, \sin \sqrt{-M_{\theta}/I} \, t$$

$$M_{\dot{\theta}} = \frac{2 I f \ell n R}{C_{y_R}}$$

$$M'_{\dot{\theta}} = M_{\dot{\theta}_w} - M_{\dot{\theta}_v} (\omega_v/\omega_w)$$

$$C_{m_q} + C_{m_{\dot{\alpha}}} = M'_{\dot{\theta}} (2 V_\infty/q_\infty A d^2)$$

2

The expression for obtaining the aerodynamic viscous-damping parameter ($M'_{\dot\theta}$) is based on the premise that the structural damping of a cross-flexure pivot varies inversely with the frequency of oscillation (Ref. 3).

The change in model oscillation frequency from the wind-off condition to the wind-on condition may be used to obtain the slope of the pitching-moment curve by the following expressions:

$$\omega = \sqrt{-M_\theta/I}$$

$$M'_\theta = M_{\theta_w} - M_{\theta_v}$$

$$M'_\theta = M_{\theta_v}\left[(f_w/f_v)^2 - 1\right]$$

$$C_{m_\theta} = M'_\theta/q_\infty Ad$$

After steady-state conditions in the tunnel had been established, the base pressure data were recorded by the automatic data system while the model was locked. The model was then displaced to an initial amplitude of approximately 3 deg (except for the 3.2-in.-diam sting where the model was displaced to approximately 2 deg) and released, with the resulting oscillatory motion being recorded on the oscillograph.

Four stings with diameter ratios (d_s/d) varying from 0.2 to 0.8 were tested. Windshields were used to vary the sting length ratio (ℓ_s/d) from 0.75 to 3.00.

Tests were conducted over a Mach number range of 2.5 to 4.0 at Reynolds numbers ranging from 0.45×10^6 to 10.2×10^6. A summary of test conditions is presented in Table 1.

5.0 PRECISION OF MEASUREMENTS

The balance was calibrated during bench tests both before and after the test, and check calibrations were made before and after each run to determine if any changes in calibration factors had occurred. The displacement calibration factor, which was obtained by use of known displacements and moments, was within ±1 percent of the maximum value of the range in which it was calibrated.

Uncertainties in the slope of the pitching-moment curve ($C_{m\theta}$) and the damping-in-pitch derivatives ($C_{mq} + C_{m\dot{\alpha}}$) occur from the following sources of error:

1. The previously mentioned error in displacement calibration.

2. Because the aerodynamic damping- and restoring-moment parameters ($M'_{\dot{\theta}}$ and M'_{θ}) are determined as the difference in wind-on and wind-off conditions.

3. The uncertainty in determining the model moment of inertia (I) and the angular frequency of oscillation (ω).

Also the damping derivatives are affected by the uncertainties in the amplitude ratio (R).

As a result of the above sources of error, the uncertainties in $C_{mq} + C_{m\dot{\alpha}}$ and $C_{m\theta}$ over the Reynolds number range presented in this report are as follows:

$M_\infty = 2.5$

Re_ℓ x 10^{-6}	1.03	4.11	7.95
$C_{m\theta}$	-0.677	-0.495	-0.604
$\Delta(C_{m\theta})$	±0.035	±0.019	±0.022
$C_{mq} + C_{m\dot{\alpha}}$	-3.51	-4.67	-3.89
$\Delta(C_{mq} + C_{m\dot{\alpha}})$	±0.22	±0.24	±0.19

$M_\infty = 3.0$

Re_ℓ x 10^{-6}	0.75	3.05	9.12
$C_{m\theta}$	-0.512	-0.532	-0.589
$\Delta(C_{m\theta})$	±0.038	±0.022	±0.022
$C_{mq} + C_{m\dot{\alpha}}$	-3.10	-4.30	-2.99
$\Delta(C_{mq} + C_{m\dot{\alpha}})$	±0.23	±0.23	±0.15

$M_\infty = 4.0$

Re_ℓ x 10^{-6}	0.91	2.73	5.34
$C_{m\theta}$	-0.529	-0.551	-0.605
$\Delta(C_{m\theta})$	±0.045	±0.025	±0.024
$C_{mq} + C_{m\dot{\alpha}}$	-2.71	-3.65	-2.97
$\Delta(C_{mq} + C_{m\dot{\alpha}})$	±0.24	±0.21	±0.16

6.0 RESULTS AND DISCUSSION

Typical experimental results are shown in Fig. 5 for $d_S/d = 0.4$ at Mach numbers 2.5, 3.0, and 4.0 for a range of Reynolds numbers and sting lengths. Theoretical values of the damping-in-pitch derivatives (first and second-order potential flow theory, Ref. 4) and of the slope of the pitching-moment curve (conical flow theory) are presented in each figure.

In addition to dynamic and static stability data, base pressure measurements were made because base pressure is very sensitive to support interference. Regarding the base pressure ratio curve for the greatest sting length ($\ell_S/d = 3.00$) as a reference (minimum support interference due to length), Fig. 5 shows that interference effects due to sting length are present. The base pressure data and schlieren photographs (Fig. 5) show that the Reynolds number range was sufficient for a transitional and fully turbulent wake. Minimum base pressure was used to indicate when transition was near the model base (Refs. 5 and 6). For $\ell_S/d = 3.00$, wake closure was obtained throughout the Reynolds number range. At $\ell_S/d = 0.75$, the wake did not attach to the sting and the base pressure increased, which therefore showed support interference.

The damping-in-pitch derivatives and the slopes of the pitching-moment curves, shown in Fig. 5, appeared to follow the variation of base pressure, i.e., the dynamic stability coefficient and the static stability derivative were a maximum and minimum, respectively, when the base pressure was a minimum. It is evident in Fig. 5 that variations in Reynolds number, which produced changes in the model boundary layer and wake, resulted in greater changes in the damping-in-pitch derivative and the static stability parameter than did the changes in the support geometry.

Figure 6 shows the dynamic and static stability parameters for the variation of sting diameter ratio (d_S/d) from 0.2 to 0.8 at Mach numbers 3.0 and 4.0 and from 0.4 to 0.8 at Mach number 2.5 for $\ell_S/d = 3.00$. Increasing the sting diameter did not produce large variations in either the dynamic stability derivative or the static stability parameter.

The theory presented in Figs. 5 and 6 shows fair agreement with the levels of the damping-in-pitch derivatives and the slopes of the pitching-moment curves.

7.0 CONCLUSIONS

Tests were conducted in Tunnel D to determine the effects of sting support interference on the dynamic and static stability characteristics of a 10-deg half-angle cone.

Data were obtained at Mach numbers 2.5 through 4.0 and at Reynolds numbers ranging from 0.45×10^6 to 10.2×10^6. Conclusions based on the results presented in this report are given below.
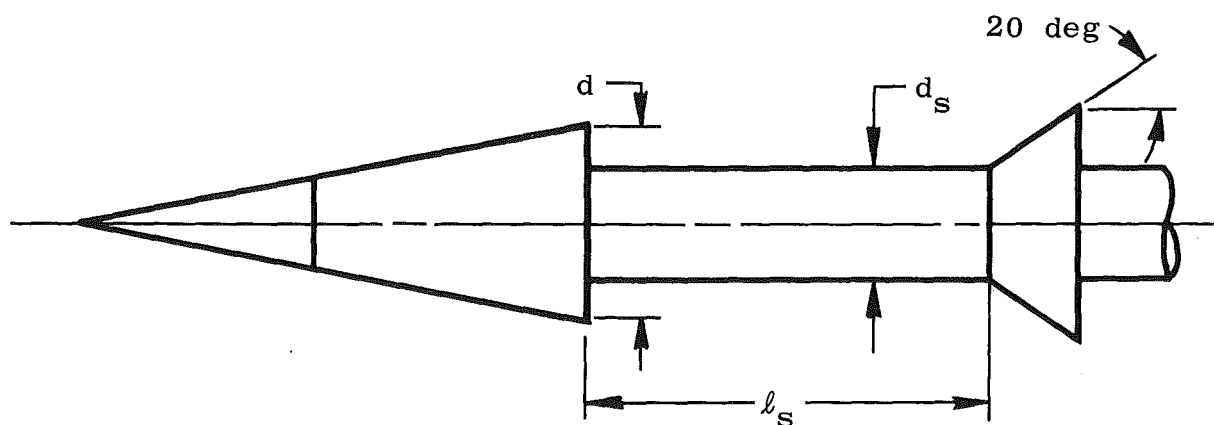
1. Variations in Reynolds number produced greater variations in the dynamic and static stability parameters than did the changes in support geometry.

2. Increasing the sting diameter from 0.4d to 0.8d at $M_\infty = 2.5$ and from 0.2d to 0.8d at $M_\infty = 3$ and 4 for $\ell_s/d = 3.00$ produced no large variations in the damping-in-pitch derivatives or in the slopes of the pitching-moment curves.
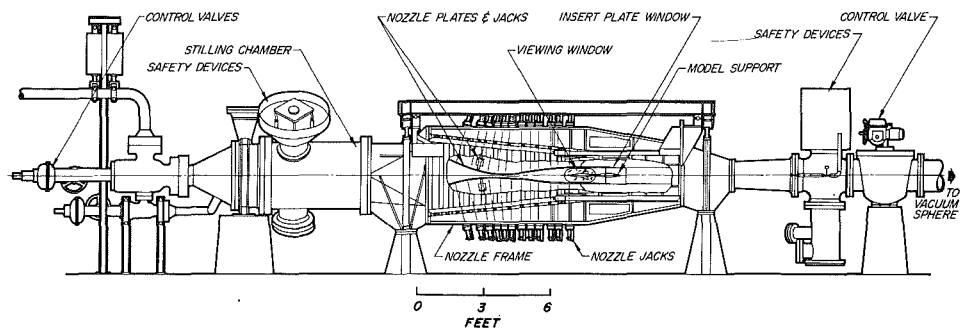
REFERENCES

1. Hodapp, Jr., A. E., Uselton, B. L., and Burt, G. E. "Dynamic Stability Characteristics of a 10-deg Cone at Mach Number 10." AEDC-TDR-64-98 (AD440188), May 1964.

2. Test Facilities Handbook (5th Edition). "von Kármán Gas Dynamics Facility, Vol. 4." Arnold Engineering Development Center, July 1963.

3. Welsh, C. J. and Ward, L. K. "Structural Damping in Dynamic Stability Testing." AEDC-TR-59-5 (AD208776), February 1959.

4. Tobak, Murray and Wehrend, William R. "Stability Derivatives of Cones at Supersonic Speeds." NACA-TN-3788, September 1956.

5. Whitfield, Jack D. "Critical Discussion of Experiments on Support Interference at Supersonic Speeds." AEDC-TN-58-30 (AD201108), August 1958.

6. Crocco, Luigi and Lees, Lester. "A Mixing Theory for the Interaction between Dissipative Flows and Nearly Isentropic Streams." Journal of Aeronautical Sciences, Vol. 19, No. 10, October 1952.
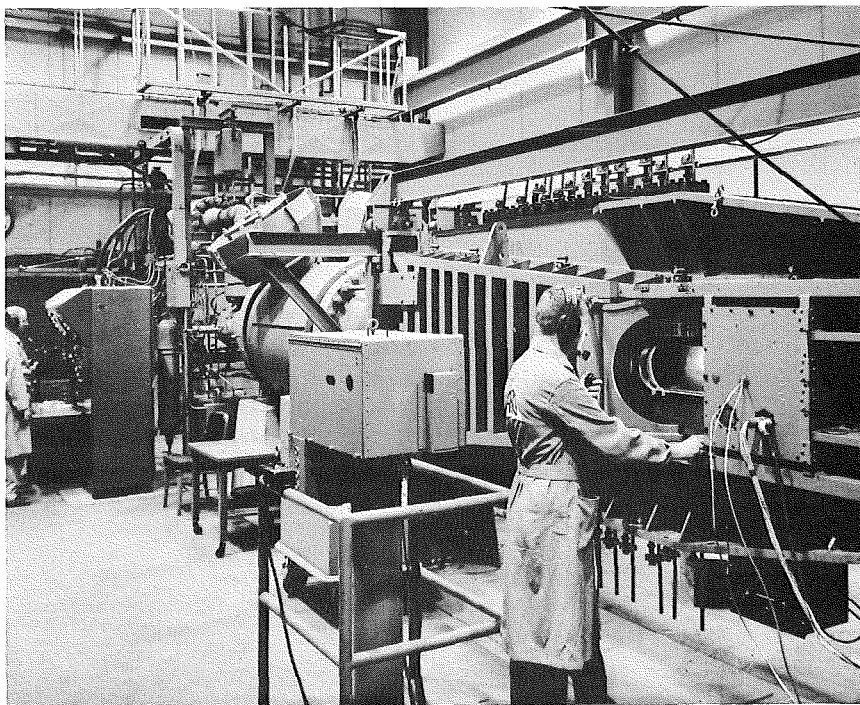
TABLE 1
TEST SUMMARY

M_∞	d_s/d	ℓ_s/d	$Re_\ell \times 10^{-6}$	θ, deg
2.5	0.4, 0.6	0.75, 1.50, 2.25, 3.00	0.98 → 10.20	±2.0
2.5	0.8	0.75, 1.50, 2.25, 3.00	0.99 → 5.95	±1.5
3.0	0.2	1.00, 2.00, 3.00	0.77 → 4.69	±2.0
3.0	0.4, 0.6	0.75, 1.50, 2.25, 3.00	0.75 → 9.25	±2.0
3.0	0.8	0.75, 1.50, 2.25, 3.00	0.75 → 6.40	±1.5
4.0	0.2	1.00, 2.00, 3.00	0.45 → 5.65	±2.0
4.0	0.4, 0.6	0.75, 1.50, 2.25, 3.00	0.46 → 5.35	±2.0
4.0	0.8	0.75, 1.50, 2.25, 3.00	0.45 → 5.35	±1.5

Assembly

Tunnel Test Section

Fig. 1 Tunnel D

Center of Gravity and
Pivot Axis Location

$\ell = 11.18$

10 deg

0.033
Spherical
Radius

$x_{cg} = 6.15$

$d = 4.00$

$x_{cg}/\ell = 0.55$

$r_n/r_b = 0.016$
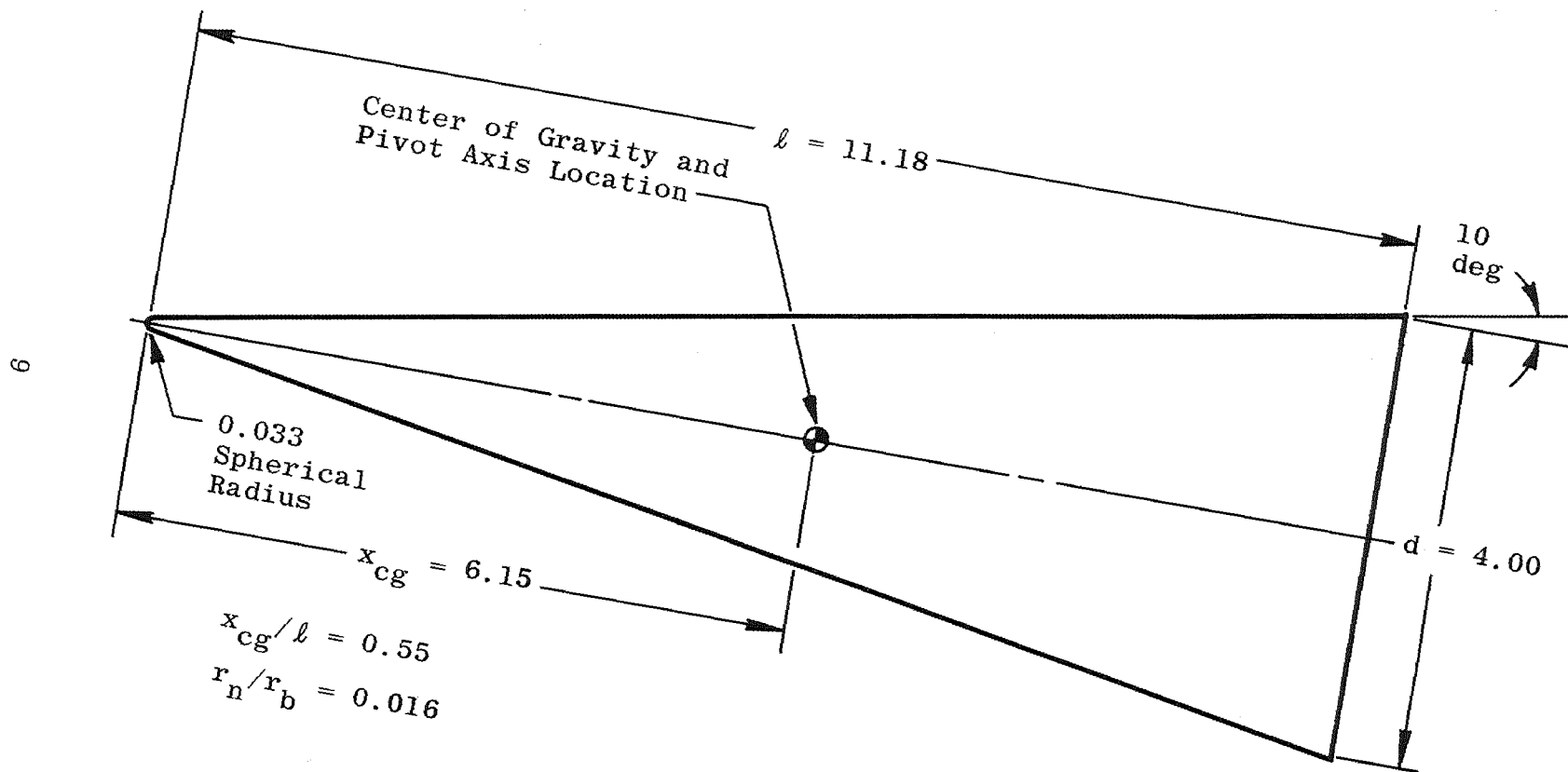
All Dimensions in Inches

Fig. 2 Model Geometry

103512
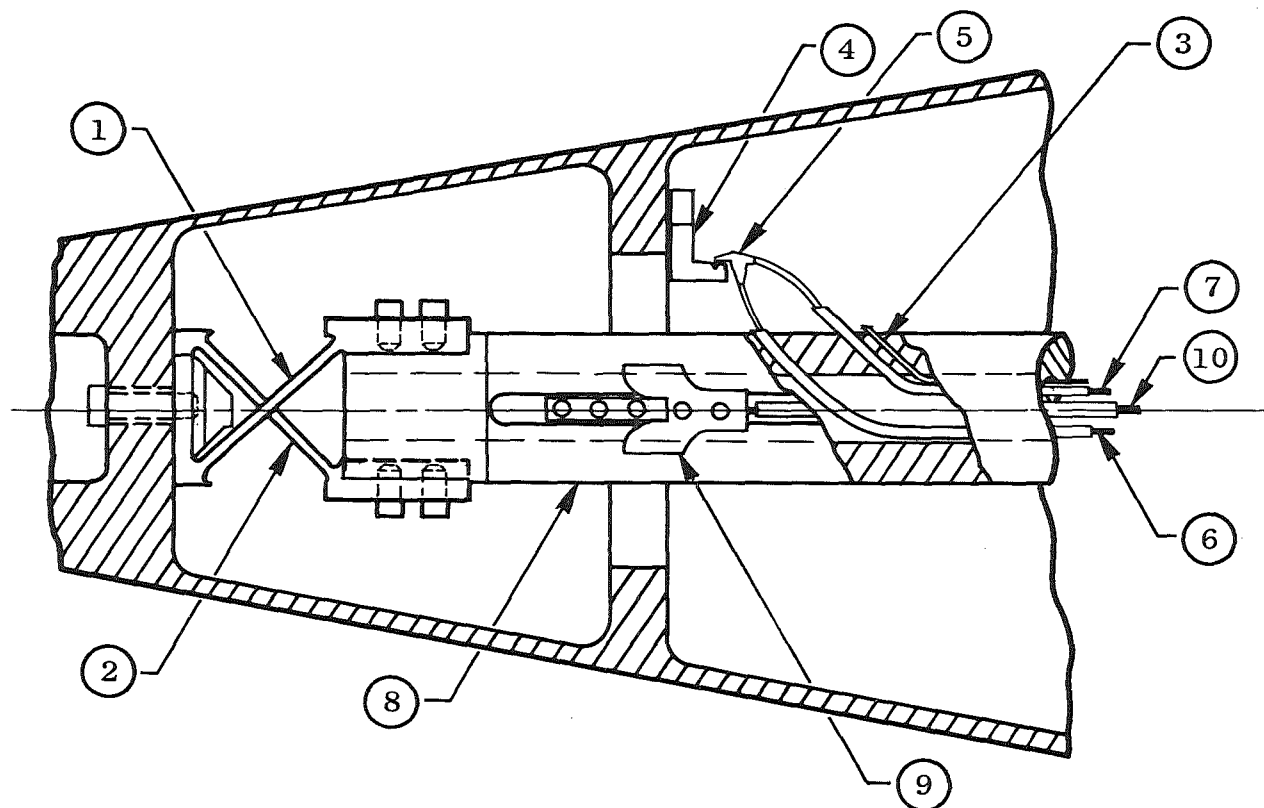
Item No.	Description	Item No.	Description
1	Side Cross-Flexure	6	Model-Displacing Cable
2	Middle Cross-Flexure	7	Model-Release Cable
3	Base Pressure Tube	8	Basic Sting
4	Model Displacement Arm	9	Trim Lock
5	Displacing Hook	10	Locking Wire

Fig. 3 Small Amplitude (±3 deg), Free Oscillation Balance
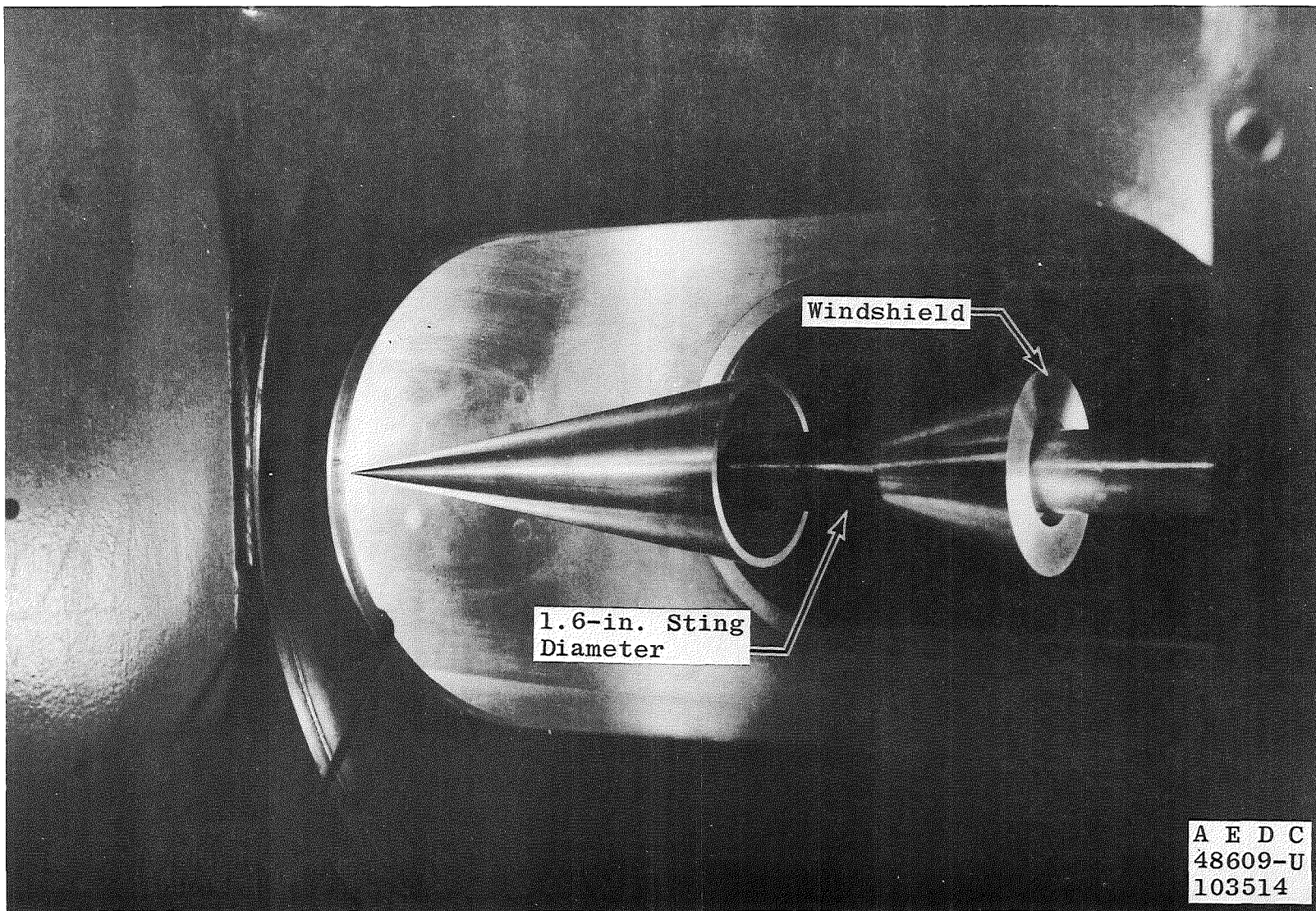
103513

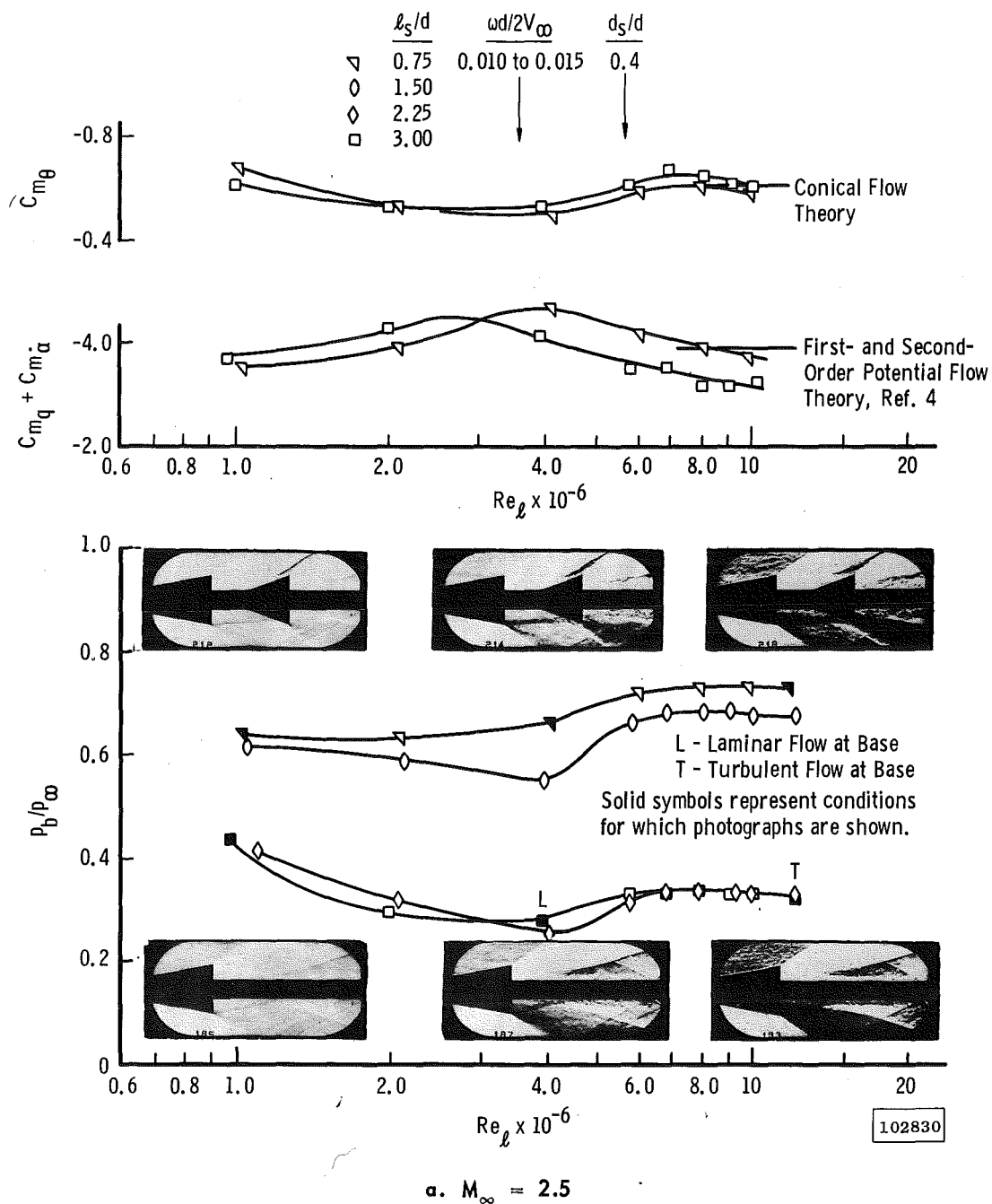Fig. 4 10-deg Cone Model ($d_s/d = 0.4$, $\ell_s/d = 0.75$) Installed in the 12-in. Supersonic Tunnel D

a. $M_\infty = 2.5$

Fig. 5 Slope of the Pitching-Moment Curve, Damping-in-Pitch Derivatives, and Base Pressure Ratio versus Reynolds Number
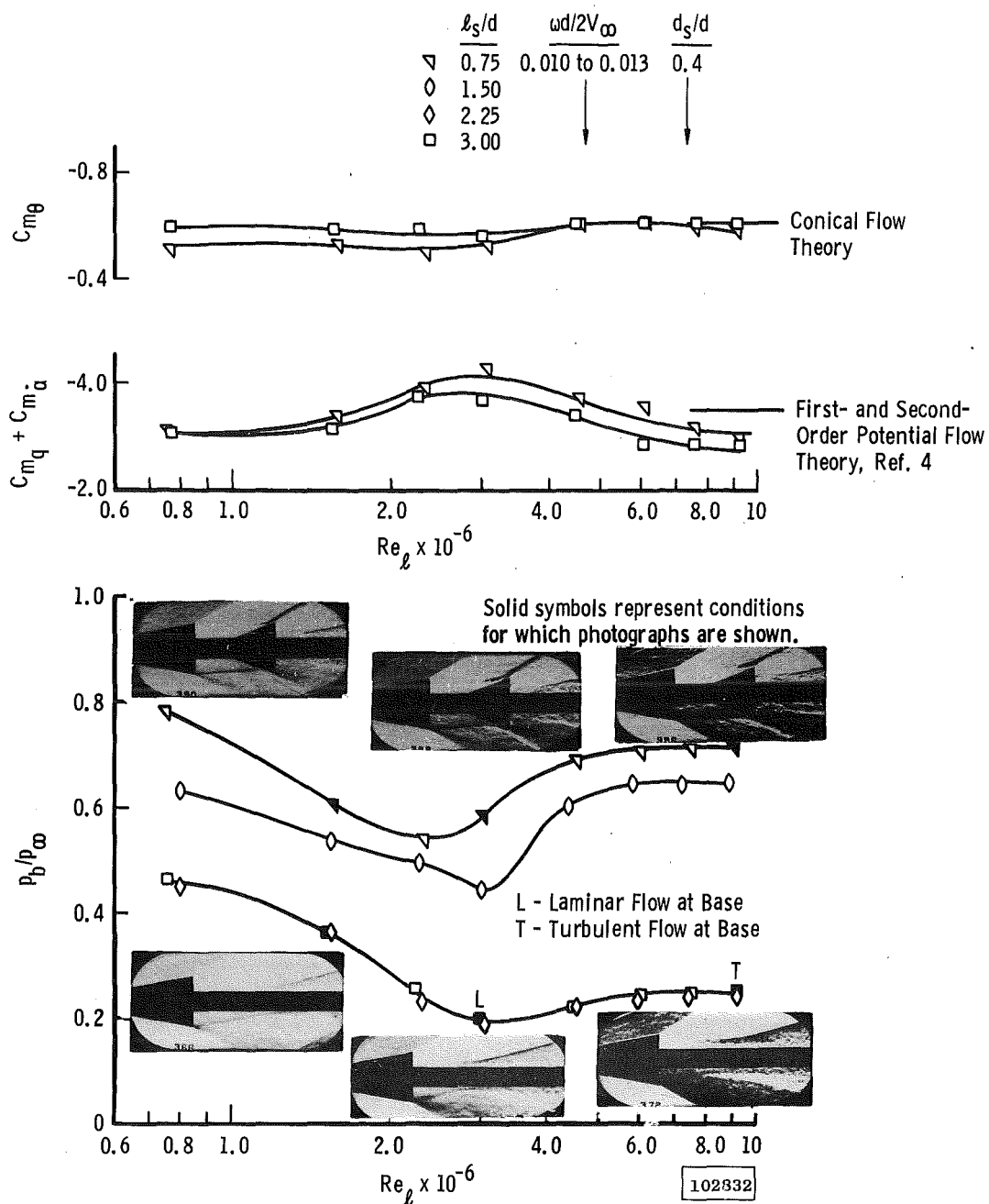
	ℓ_S/d	$\omega d/2V_\infty$	d_S/d
◁	0.75	0.010 to 0.013	0.4
◊	1.50		
◊	2.25		
□	3.00		

Conical Flow Theory

First- and Second-Order Potential Flow Theory, Ref. 4

Solid symbols represent conditions for which photographs are shown.

L – Laminar Flow at Base
T – Turbulent Flow at Base
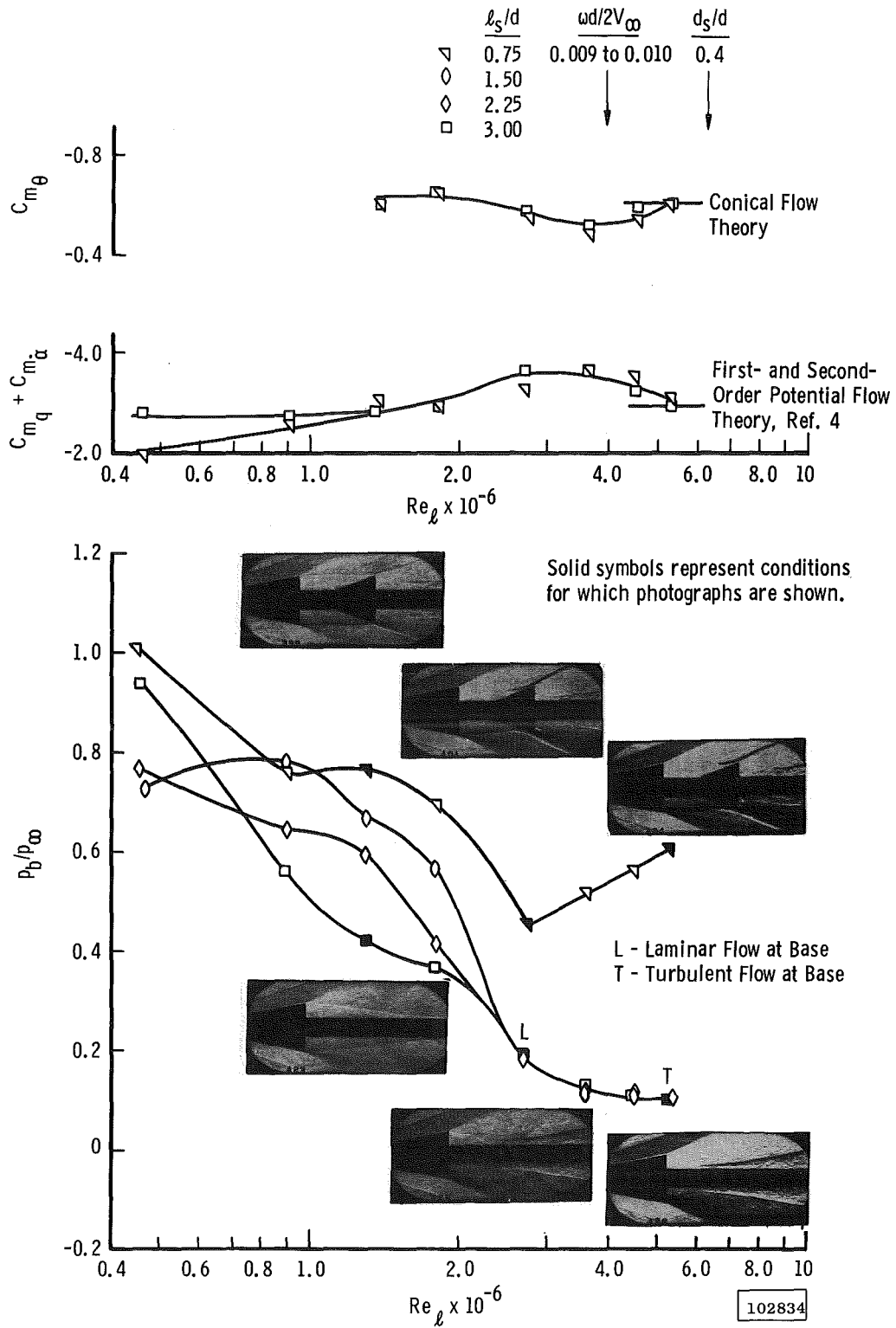
102832

b. $M_\infty = 3.0$
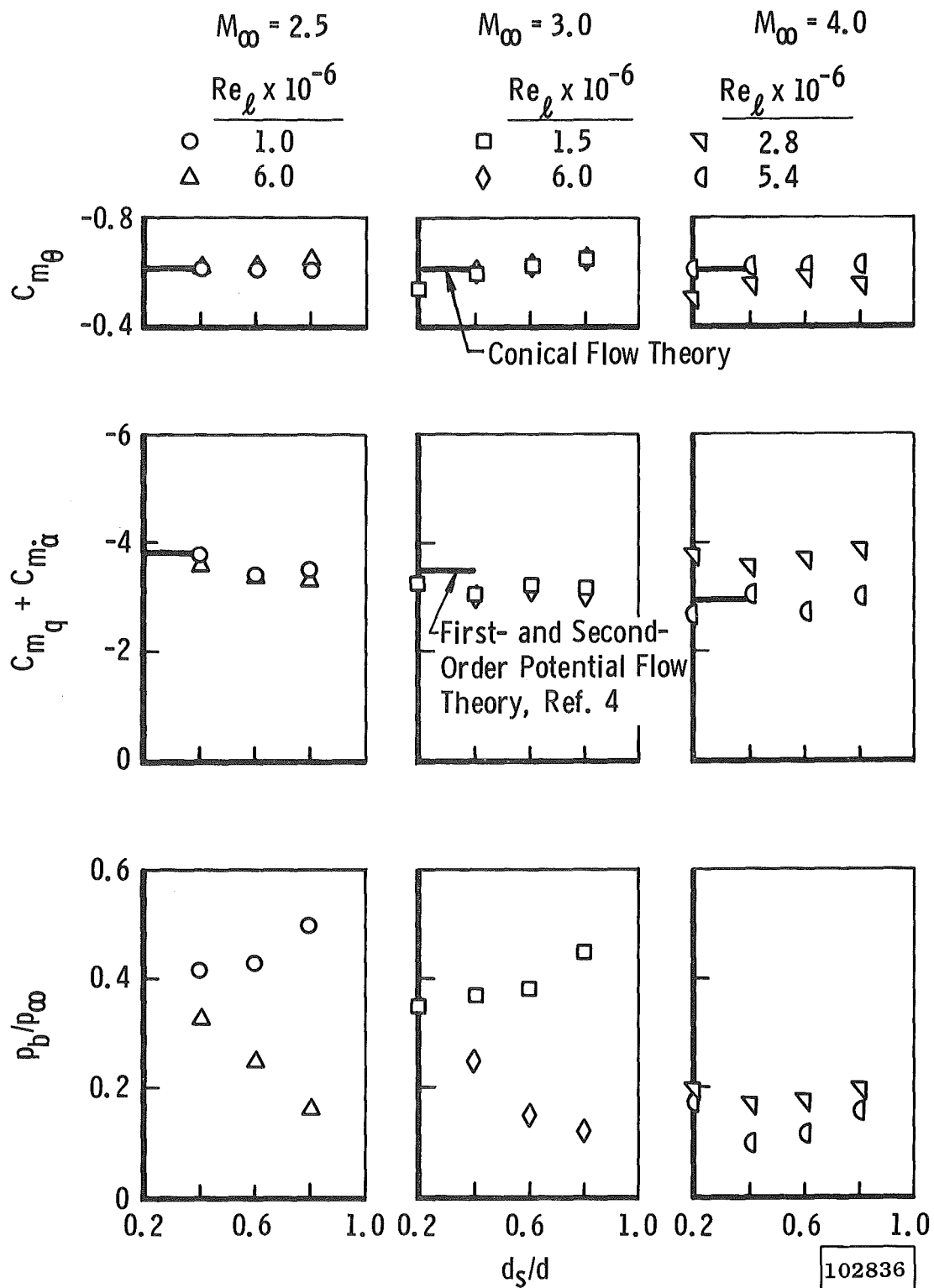
Fig. 5 Continued

c. $M_\infty = 4.0$

Fig. 5 Concluded

Fig. 6 Slope of the Pitching-Moment Curve, Damping-in-Pitch Derivatives, and Base Pressure Ratio versus Sting Diameter Ratio for $\ell_s/d = 3$

102836